Single- and Double-Shelled Coaxial Nanocables of GaP with Silicon Oxide and Carbon†

Seung Yong Bae, Hee Won Seo, Hyun Chul Choi, Doo Suk Han, and Jeunghee Park*

Department of Chemistry, Korea University, Jochiwon 339-700, S. Korea

Received: August 4, 2004; In Final Form: November 17, 2004

Coaxial nanocables of gallium phosphide (GaP) core with three different-typed single and double shells (i.e., silicon oxide (SiO_x), carbon (C), and SiO_x/C) were exclusively synthesized by the chemical vapor deposition method. The GaP/SiO_x nanocables were directly grown on gold-deposited silicon substrates. Deposition of C on the GaP nanowires and GaP/SiO_x nanocables produces the GaP/C and GaP/SiO_x/C nanocables, respectively. The outer diameter of the nanocables is <50 nm. The thickness and crystallinity of the C outer layers were controllable by the growth conditions. X-ray photoelectron spectroscopy, X-ray diffraction, Raman spectroscopy, and photoluminescence reveal that the outer layer formation reduces the surface defects of GaP nanowires. A great enhancement of the conductivity due to the C outer layers has been measured by the four-probe method. The growth process of these nanocables has been discussed on the basis of the vapor−liquid−solid mechanism.

1. Introduction

Since the discovery of carbon nanotubes (CNTs), one-dimensional (1D) nanostructures have attracted much attention as well-defined building blocks to fabricate nanoscale electronic and optoelectronic devices.[1−5] The formation of semiconductor heterostructures is believed to be of importance in tailoring the optical, electronic, electrical, magnetic, and chemical properties of 1D nanostructures. The diverse heterostuctures with modulated compositions and interfaces include nanowire heterojunctions,[6−9] superlattices,[10−12] nanotapes,[13] biaxial nanowires,[14] and coaxial nanocables.[15−44] In particular, many different coaxial nanocables have been synthesized by a large number of research groups.[15−44] Indeed, they have already demonstrated the great potential in nanodevice applications such as coaxial-gated transistors and laser diodes.[11b,16,21c]

One of the important wide band-gap semiconductors, gallium phosphide (GaP), is a potential material for optical and high-temperature electronic devices. The band-gap energy (E_g) is 2.24 eV at 300 K. The GaP nanorods, nanowires, and nanobelts were synthesized by laser ablation,[45,46] carbon nanotube-confined reaction,[47] thermal decomposition in the presence of surfactants,[48] and evaporation or sublimation methods.[49−52] Duan and Lieber first reported the synthesis of GaP nanowires using a laser-assisted catalytic growth method in which the pulses of a 1064-nm Nd:YAG laser ablates an Au-containing GaP target.[45] Shi et al. synthesized the GaP nanowires by the laser ablation method in which the GaP/Ga_2O_3 target was irradiated by pulsed 248-nm KrF laser.[46] Tang et al. used the reaction of carbon nanotubes with a Ga/Ga_2O_3 mixture in a phosphorus vapor atmosphere.[47] The GaP nanorods were synthesized by thermal decomposition of tris(di-*tert*-butylphosphino)gallane in amine stabilizers.[48] Lyu et al. used an evaporation of a Ga/GaP mixture to produce the oxide-layer-coated GaP nanowires.[49] Our group synthesized the GaP nanowires and nanobelts via a sublimation of ball-milled GaP powders under argon (Ar) or ammonia (NH_3) atmosphere.[50−52] Despite such successful syntheses of GaP nanowires, however, there are only a few reports on the heterostructure of GaP nanowires. Gudiksen et al. reported the synthesis of GaP/GaAs nanowire superlattices using a laser-assisted catalytic growth method and showed their unique photonic and electronic properties.[11] Lin et al. synthesized the GaP core/GaN shell structure by the chemical vapor deposition (CVD) method.[30]

In this paper, we first report the synthesis of three different core−shell nanocables, GaP/SiO_x, GaP/C, and GaP/SiO_x/C, with selective morphology and structure. We developed the thermal CVD method by modifying the experimental conditions used for the synthesis of GaP nanowires in which the ball-milled GaP powders sublimate under Ar flow at 1000−1100 °C.[50] The electrical properties of SiO_x and C outer layers are expected to be insulating and metallic, respectively. These nanocables would certainly diversify the application of GaP nanowires in the electronic or optoelectronic nanodevice fabrication. However, to utilize the nanocables, it would be essential to have detailed information about the crystal/surface structure that is responsible for the band-gap energy as well as optical properties. The ultimate goal of the present study is to find the effect of coating on the structural properties of GaP nanowires using various spectroscopic techniques.

2. Experimental Section

GaP (99.99%, Aldrich) pieces were milled using a mechanical-ball mill system for 20 h. The Si substrates were coated with 0.001 M $HAuCl_4 \cdot 3H_2O$ (98+%, Sigma) ethanol solution, leading to the deposition of Au nanoparticles. For the synthesis of GaP/SiO_x nanocables, the ball-milled GaP powders and a piece of Si wafer as the Si source were placed in a quartz boat located inside a quartz tube reactor. The substrate was positioned at a distance of about 15 cm from the source. The source was sublimated under Ar flow at a rate of 500 standard cubic centimeters per minute (sccm). The temperature of the source was set at 1000−1100 °C, and that of the substrate was approximately 700−800 °C. The growth time was 10−30 min. For the C deposition on the GaP nanowires, the ball-milled GaP powders sublimated under Ar flow at 1000−1100 °C, and then

† Part of the special issue "George W. Flynn Festschrift".

* E-mail: parkjh@korea.ac.kr.

10.1021/jp046501e CCC: $30.25
Published on Web 02/12/2005

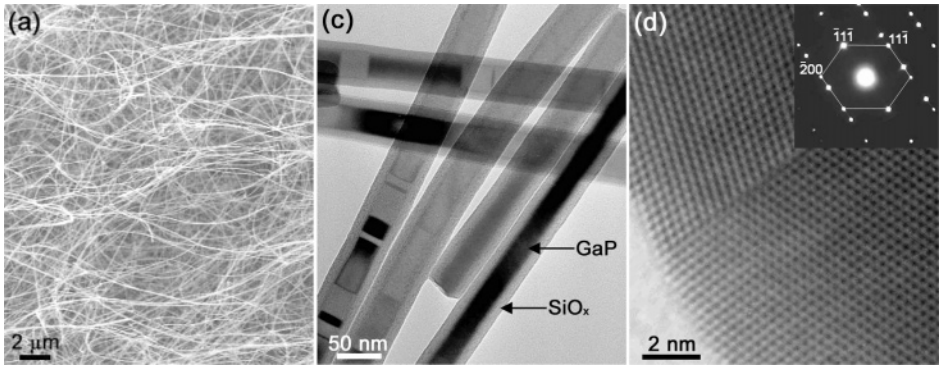

Figure 1. (a) SEM micrograph of the high-density wirelike nanostructures. (b) TEM image reveals the GaP/SiO_x coaxial nanocable structure. (c) Atomic-resolved image shows twin-crystalline zinc-blende structured GaP nanowire core. Its corresponding SAED pattern confirms the [111] growth direction (inset).

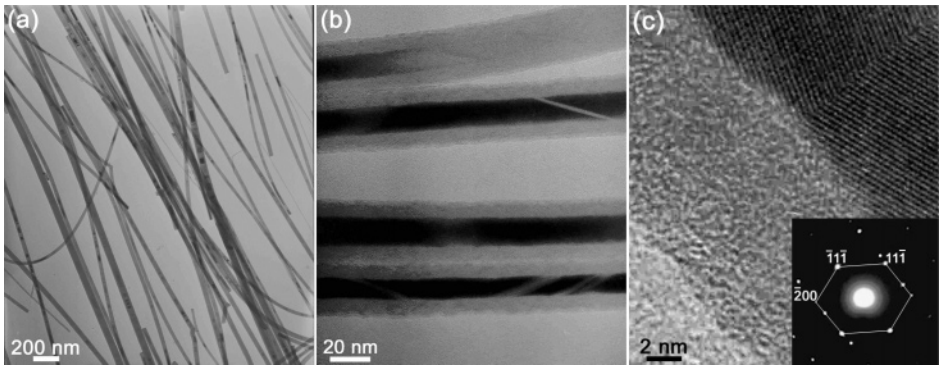

Figure 2. (a) TEM image shows the uniform diameters of the GaP/C nanocables. (b) The nanowires are sheathed homogeneously with the C outer layers. (c) Atomic-resolved image reveals zinc-blende GaP nanowire core and the amorphous C outer layers. The corresponding SAED pattern confirms the [111] growth direction (inset).

CH_4 or C_2H_2 flowed at a rate of 20−50 sccm for 1−5 min. For the synthesis of GaP/SiO_x/C nanocables, the pregrown GaP/SiO_x nanocables were placed inside the reactor and CH_4 or C_2H_2 flowed with a rate of 20−50 sccm for 1−5 min. The temperature was set at 850−950 °C. Wool-like product deposits on a large area of the substrate. The color of products is usually light yellow, but it is dark yellow when the C deposition occurs.

The size, structure, and composition of the products were examined by scanning electron microscopy (SEM, Hitachi S-4300), high-resolution transmission electron microscopy (TEM, JEOL JEM-2010, 200 kV), electron diffraction (ED), energy-dispersive X-ray spectroscopy (EDS), electron energy-loss spectroscopy attached to TEM (Philips CM200), and powder X-ray diffraction (XRD, Philips X'PERT MPD). XPS measurements were performed at the 8A1 (Undulator U7) beam line of the Pohang-Light-Source. Raman spectroscopy (Renishaw RM1000) was carried out using a 514.5-nm argon ion laser. The photoluminescence (PL) measurement was conducted using the 458-nm line of an argon ion laser as an excitation wavelength. The laser power was 1 kW/cm^2. The wavelength was precisely calibrated using the atomic lines from an argon calibration lamp. The conductivity of GaP nanowires and nanocables deposited on the substrates was measured by the four-probe method with an HP4156 parameter analyzer at room temperature.

3. Results

3.1. Synthesis of GaP/SiO_x Nanocables. Figure 1a shows an SEM image of the high-density wirelike nanostructures. The length is up to 500 μm. The TEM image reveals the nanocable morphology in which the layers homogeneously coat the straight nanowires along the entire length (Figure 1b). The diameter distribution is narrow, in the range 30−40 nm. The end is flat and open without the outer layers. The nanocables are rotated on the grid, showing that the diameter is not changed much. The outer diameter of the nanocables is uniformly 40−50 nm, and the thickness of the outer layers is about 10 nm. The EDX analysis identifies Ga and P with atomic ratio of nearly 1:1 (see Supporting Information Figure S1). The significant atom % of Si and O components are detected. The C and Cu components have originated from the C-coating Cu TEM grid. High-resolution TEM (HRTEM) imaging reveals that the core consists of the zinc-blende structured GaP crystal with a twin boundary perpendicular to the wire axis (Figure 1c). Most of the nanocables exhibit lines perpendicular to the wire axis, corresponding to the twin structure, as shown in Figure 1b. The (111) fringes perpendicular to the wire axis are separated by about 3.1 Å, which is consistent with that of the GaP crystal (a = 5.4506 Å; JCPDS card no. 32-0397). The SAED pattern further confirms the [111] growth direction (inset).

3.2. Synthesis of GaP/C Nanocables. Wire-like nanostructures produced by a subsequent CVD of CH_4 following the growth of GaP nanowires. TEM image reveals the nanocable morphology in which the straight nanocables are homogeneously produced (Figure 2a). A magnified image reveals the cable structure in which the layers uniformly coat the nanowires (Figure 2b). The diameter distribution is narrow, in the range 30−40 nm. The thickness of the outer layers is uniformly 10 nm, and the average diameter of the core is 15 nm. An atomic-resolved image reveals that the GaP core is nearly single-crystalline with a few defects, and the outer layers are amorphous (Figure 2c). The SAED pattern further confirms the zinc-blende structure and the [111] growth direction of the GaP nanowire core (inset). The EDX analysis identifies the 1:1 ratio

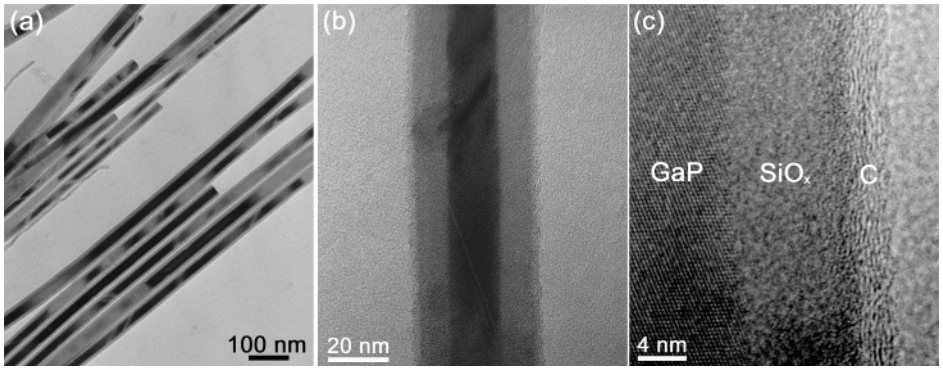

Figure 3. (a) TEM image shows the GaP/SiO_x/C nanocables. (b) The outer layers sheath the GaP nanowire with uniform thickness. (c) Atomic-resolved image reveals the crystalline GaP crystal, amorphous SiO_x layers, and graphitic outer layers.

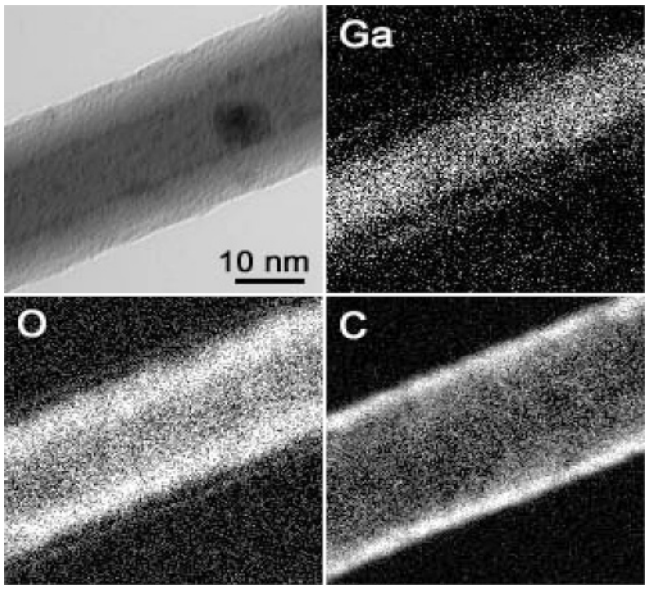

Figure 4. TEM image of a selected GaP/SiO_x/C nanocable and its elemental maps of Ga, O, and C, obtained by EELS imaging using inelastic electrons corresponding to the energy loss of each element.

of Ga/P and a large amount of C component (see Supporting Information Figure S1). Raman spectrum analysis (section 3.6) reveals that the amorphous outer layers are composed of C.

3.3. Synthesis of GaP/SiO_x/C Nanocables. The graphitic outer layers were produced on the pregrown GaP/SiO_x nanocables via a CVD of C_2H_2 at 900 °C. Figure 3a shows a TEM image of GaP/SiO_x/C nanocables in which all GaP nanowires are sheathed with the outer layers. They have smooth surfaces without any impurities. Both ends of the nanocables are flat and nearly open with negligible outer layers. The average outer diameter is 50 nm. The EDX analysis identifies Ga, P, Si, C, and O components (see Supporting Information Figure S1). Figure 3b corresponds to the TEM image of a typical nanocable, showing that the outer layers homogeneously sheath the GaP nanowire. Its atomic-resolved image reveals that the single-crystalline GaP nanowire is sheathed with the amorphous SiO_x layers and surrounded again with the graphitic layers (Figure 3c). The diameter of the GaP nanowire is 15 nm, and the thicknesses of the SiO_x inner shell and graphitic outer shell are 10 and 2 nm, respectively. The fringes of the graphitic sheets are separated by 0.34 nm. The thickness of graphitic layers can be controlled by the C deposition time.

Figure 4 displays the EELS (or energy-filtered TEM) imaging of a GaP/SiO_x/C nanocable whose outer diameter is 30 nm. The corresponding TEM image is shown in the top left figure. The elemental mapping of Ga was obtained using the energy loss

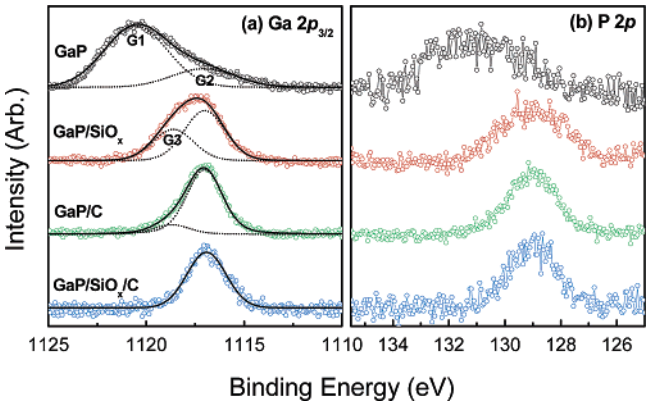

Figure 5. The fine XPS spectrum of (a) Ga $2p_{3/2}$ and (b) P 2p. The Ga $2p_{3/2}$ band is deconvoluted into two bands G1 and G2 (dotted lines) for GaP nanowires and G2 and G3 bands (dotted lines) for GaP/SiO_x and GaP/C nanowires. Open circles and lines correspond to the data points and the sum of the deconvoluted bands, respectively.

of L-shell edges ($L_{2,3}$) ($\Delta E = 1115$ eV). The O and C elemental mapping uses the energy loss of K-shell edges of O ($\Delta E = 532$ eV) and C ($\Delta E = 283.0$ eV), respectively. The elemental mapping of P and Si is not displayed, because the peaks of Si $L_{2,3}$ ($\Delta E = 99.2$ eV) and P $L_{2,3}$ ($\Delta E = 132.2$ eV) are nearly overlapped and the energy filtering was not very successful. The brighter points represent a higher concentration of the element, showing that Ga consists of only a core part, and the O and C components exist at the inner shell and outer shell, respectively. This elemental mapping confirms that the C layers definitely sheath the O-containing layers.

3.4. Fine XPS Spectrum of Ga and P. The XPS survey scan spectrum has been measured for GaP nanowires, and all three GaP/SiO_x, GaP/C, and GaP/SiO_x/C nanocable samples used photon energy of 1265 eV. The GaP nanowires were synthesized by the sublimation method.[50] The fine XPS spectrum of Ga $2p_{3/2}$ is displayed in Figure 5a. The gap between Ga $2p_{3/2}$ and Ga $2p_{1/2}$ is 26.8 eV, which agrees with the reference value of 26.84 eV.[53] The peak width of four samples follows the order GaP $\gg$ GaP/SiO_x $>$ GaP/C $\approx$ GaP/SiO_x/C. In the case of GaP nanowires, the broad band is deconvoluted into two bands, G1 at 1120.5 eV and G2 at 1117.0 eV. We assign the strong, broad G1 band to the Ga in many different bonding states at the surface region, including the Ga−O dangling bonds and the Ga bonded to the doped O. The G2 band is assigned to the Ga bonded to P (Ga−P). For GaP/SiO_x and GaP/C nanowires, the band can be deconvoluted into two bands, G3 at 1118.7 eV and G2 at 1117.0 eV. The G3 band is attributed to the Ga bonded to the doped O atoms. The significant G3 band of GaP/SiO_x nanocables is most likely due to the interface between GaP nanowires

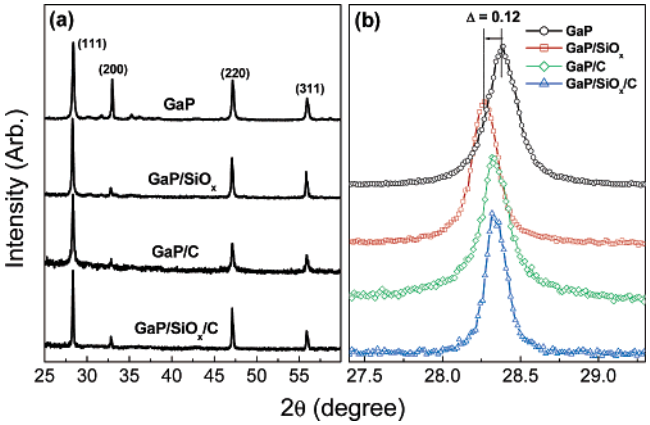

Figure 6. (a) Full-range XRD pattern of GaP nanowires, GaP/SiO_x, GaP/C, and GaP/SiO_x/C nanocables. (b) Magnified (111) peak showing the peak shift and broadening.

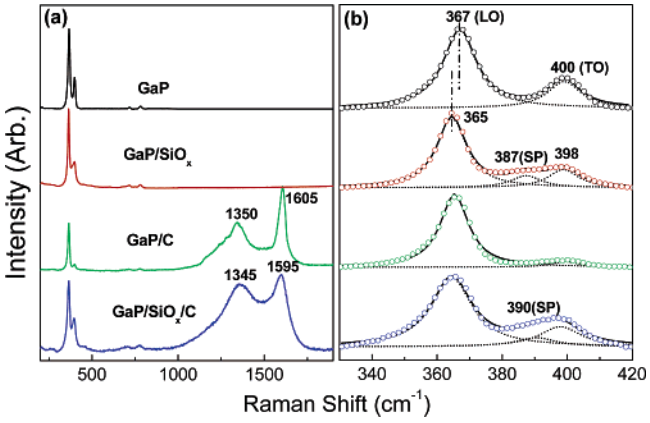

Figure 7. (a) First-order Raman scattering spectrum of GaP nanowires, GaP/SiO_x, GaP/C, and GaP/SiO_x/C nanocables. (b) Magnified LO and TO mode region. The band deconvoluted into LO, TO, and SP bands (dotted lines). Open circles and lines correspond to the data points and the sum of the deconvoluted bands, respectively. The excitation wavelength is 514.5 nm from an argon ion laser.

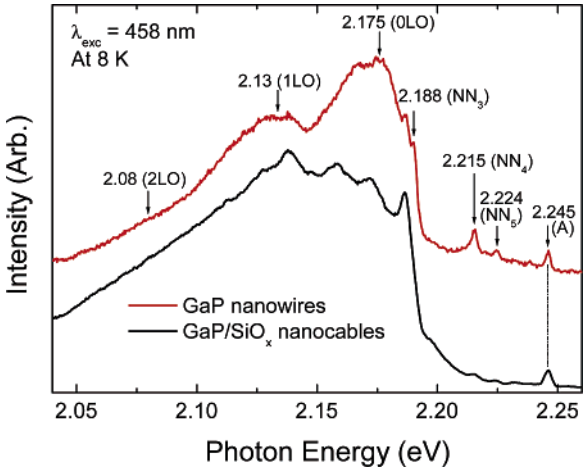

Figure 8. PL spectrum of the GaP nanowires and GaP/SiO_x nanocables measured at 8 K. The excitation wavelength is 458 nm from an argon ion laser.

and SiO_x outer layers. However, the SiO_x and C outer layers can eliminate the Ga−O dangling bonds, so the intensity and width of the G3 band is much lower than those of the G1 band. The spectrum of GaP/C and GaP/SiO_x/C nanocables consists of mainly the Ga−P band. The complete disappearance of the G3 band in the GaP/SiO_x/C nanocables is related to the annealing of GaP nanowires during C deposition on the SiO_x outer layers.

The finely scanned P 2p peak is shown in Figure 5b. The peak width of the nanocables is narrower than that of the GaP nanowires. The peak broadening follows the same order as that of the Ga $2p_{3/2}$ peak. For GaP nanowires, the abundant P−O dangling bonds at the surface would contribute to the large peak broadening. The outer layers protect the GaP nanowires from drastically reducing the number of dangling bonds.

3.5. XRD Patterns. Figure 6ashows the full-range XRD pattern of GaP nanowires and nanocables. All peaks correspond to those of cubic GaP crystal (JCPDS card no. 32-0397). The magnified (111) peak is displayed in Figure 6b. All nanocables exhibit a narrower peak width than the GaP nanowires. This result can be interpreted by the reduction of dangling bonds at the surface of GaP nanowires, as we discussed in the XPS data. The GaP/SiO_x nanocables show a peak shift to the lower angle by 0.12° from that of GaP nanowires. The crystal defects, such as twin structure, as well as the O doping may be responsible for the increase in the lattice constant of GaP. As the C outer layers deposit on the GaP/SiO_x nanowires, the peak shifts slightly to the higher angle and the width becomes narrower. The elimination of doped O atoms following the annealing of the GaP crystal would result in a decrease of lattice constants, which is rationalized by the XPS data.

3.6. Raman Spectrum. Figure 7a shows the first-order Raman spectrum of GaP nanowires and nanocables. They commonly show the first-order phonon frequencies of transverse optical (TO) and longitudinal optical (LO) modes at about 365 and 398 cm^{-1}, respectively.[54] Figure 7b corresponds to the magnified TO and LO mode peaks, revealing that the peak position of the GaP nanocables is 2 cm^{-1} lower than that of the GaP nanowires. The peak shift to the lower frequency region indicates the more defective crystal structure of GaP nanocables. Recently, a peak on the left side of the LO mode peak was assigned to the surface phonon (SP) mode of the GaP nanowires.[55,56] It was suggested that the frequency is sensitive to the dielectric constant of the surrounding medium in which the nanowire is imbedded. The spectrum was fit into the three bands LO, TO, and SP. The GaP nanowires and GaP/C nanocables show a negligible SP mode. In contrast, the GaP/SiO_x and GaP/SiO_x/C nanocables show the SP mode at 387 and 390 cm^{-1}, respectively, which may be related to a high dielectric constant of the SiO_x outer layers.

The first-order Raman peak of C usually consists of three bands at ∼1350 cm^{-1} (D band), ∼1580 cm^{-1} (G band), and ∼1605 cm^{-1} (D′ band).[57] The origin of the D and D′ bands has been explained as disorder-induced features due to the finite particle size effect or lattice distortion. The G band originates from the Raman-active E_{2g} mode due to in-plane atomic displacements. Two bands of GaP/C nanocables at 1345 and 1605 cm^{-1} can be assigned to the D and D′ bands, respectively, indicating the amorphous phase of the C outer layers. For the GaP/SiO_x/C nanocables, the G and D′ bands overlap to one band at 1595 cm^{-1}. The appearance of the G band indicates the crystalline phase of the C outer layers.

3.7. PL Spectrum. We were able to measure the PL spectrum of GaP/SiO_x nanocables at 8 K and plotted with that of GaP nanowires (Figure 8). In the spectrum of GaP nanowires, two broad bands at 2.175 and 2.13 eV and a shoulder at 2.08 eV are assigned to the donor−acceptor pair (DAP, 0LO) peak and its replicas (1LO and 2LO).[50] In the spectrum of GaP/SiO_x nanowires, these DAP bands are almost overlapped. It could be caused by the increased level of impurities, such as the O

TABLE 1: Conductivity Data of GaP Nanowires and Nanocables

samples	resistance (Ω)	conductivity (S/cm)[a]
GaP nanowires	1.2×10^{8}	2.8×10^{-6}
GaP/SiO_x nanocables	3.6×10^{11}	9.3×10^{-10}
GaP/C nanocables	4.7×10^{2}	0.71
GaP/SiO_x/C nanocables	5.4×10^{2}	0.62

[a] Spacing between tips: 30 μm.

doping, that occurs at the interface region. The peak at 2.245 eV (labeled A) originates from the recombination of isoelectronic excitons bound to isolated N atoms in GaP. The GaP nanowires show peaks at 2.188, 2.215, and 2.224 eV, labeled as NN_3, NN_4, and NN_5, respectively, arising from the recombination of isoelectronic excitons bound to the N atom pairs. The appearance of these peaks indicates that the N atoms would remain at the surfaces of the nanowires because of the adsorption of air and the N atom concentration above 10^{17} cm^{-3}. The GaP/SiO_x nanowires exhibit only the A band, indicating that the N atom concentration at the surface is much lower than that of the GaP nanowires. The SiO_x outer layers should protect the GaP nanowires from the adsorption of air, as expected from the results of XPS and XRD.

3.8. Influence of the C Outer Layers on the Conductivity of GaP Nanocables. Conductivity measurements have been carried for the GaP nanowires, GaP/SiO_x nanocables, GaP/C nanocables, and GaP/SiO_x/C nanocables deposited on the Si substrate. Table 1 lists the resistance (Ω) and the conductivity (S/cm) of the samples. The standard four-probe technique was used, and the spacing of tips was 30 μm. The conductivity of the GaP nanowire and GaP/SiO_x nanocable network is extremely low. The SiO_x outer layers result in much lower conductivity. As the graphitic outer layers encapsulate these nanowires and nanocables, the conductivity is greatly enhanced by factors of 10^5 and 10^9, respectively. The C-encapsulated nanocables have a conductivity of 0.6−0.7 S/cm, exhibiting nearly metallic properties. It agrees with an intrinsically high conductivity of the graphitic layers, which means that the contact resistance of inner nanocables is much reduced compared to the GaP nanowires and GaP/SiO_x nanocables.

4. Discussion

A schematic diagram for the growth process of (i) GaP nanowires, (ii) GaP/SiO_x nanocables, (iii) GaP/C nanocables, and (iv) GaP/SiO_x/C nanocables has been drawn as shown in Figure 9. The SEM analysis reveals the formation of 30−80 nm Au nanoparticles deposited on the substrates at the growth temperature. When only ball-milled GaP powders are sublimated, the GaP nanowires are grown up from these Au nanoparticles that are presumably saturated with Ga and P, following a vapor−liquid−solid (VLS) mechanism. The average diameter of GaP nanowires is 50 nm. For the formation of SiO_x outer layers, the Si wafer is used as an Si source. The Si wafer can melt with GaP (actually Ga) at the source temperature of 1000−1100 °C and supply the Si vapor.[58] The Si, SiO_x, and SiC nanowires were synthesized using the dissolved Si wafers in molten Ga.[59−61] The Si vapor would dissolve into the Au nanoparticles on substrates and form a eutectic melting with Au and also Ga at the growth temperature (700−800 °C). So, the SiO_x outer layers may be grown simultaneously with the GaP nanowires, following the VLS mechanism. The outer diameter of the nanocables is 45 nm, which is similar to the GaP nanowires. This rationalizes the VLS growth mechanism we proposed. The one-step synthesis of the SiO_x outer layers

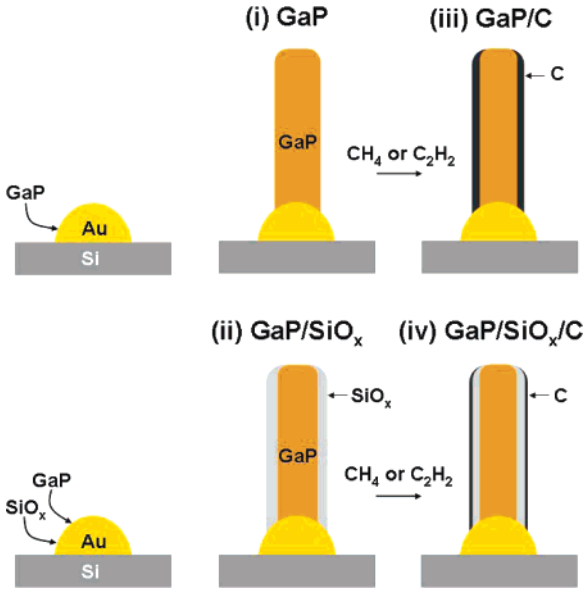

Figure 9. A schematic diagram for the growth process of (i) GaP nanowires, (ii) GaP/SiO_x nanocables, (iii) GaP/C nanocables, and (iv) GaP/SiO_x/C nanocables.

has been previously reported for Si, Ge, SiC, InS, In_2S_3, CdSe, ZnO, and so forth.[17b−e,18k,39,40,44]

For C deposition on the GaP nanowires, we used a one-step CVD method in which CH_4 or C_2H_2 flows just after the sublimation of GaP powders by Ar flow. The GaP nanowires grow first, and the deposition of amorphous C layers would occur on the grown GaP nanowires. When C deposition takes place at the same temperature as that of the GaP nanowires (700−800 °C), the amorphous phase of C outer layers is inevitable because of the low temperature. It is well-known that the degree of crystalline perfection of the graphitic sheets increases with the temperature. We previously reported a direct synthesis of the SiC/C nanocables using a CVD method in which CH_4 flows after the growth of SiC nanowires at 1100 °C, and the crystalline C layers form surrounding the SiC nanowires.[24b] Therefore, we employed a two-step route that deposits the crystalline C layers on the pregrown GaP/SiO_x nanocables at a temperature above 800 °C. The formation of graphite layers was successful at 850−900 °C. At a temperature higher than 950 °C, the GaP/SiO_x nanocables were destroyed before C deposition, probably because of oxidation with residual air. We could not achieve the deposition of graphite outer layers on the pregrown GaP nanowires using the same procedure. The reaction of C source attacking the GaP nanowire surface starts after C deposition begins. The SiO_x outer layers apparently protect the GaP nanowire core from such a reaction. This can be rationalized by the diameter of the nanocables. The diameter of GaP nanowires is 50 nm, but the diameter of the GaP nanowire core in the GaP/C nanocables is usually 15 nm. In the case of GaP/SiO_x/C nanocables, the diameter of GaP/SiO_x nanocables is not greatly reduced.

HRTEM images and SAED patterns of GaP/SiO_x and GaP/C nanocables show the twin structure that cannot be observed from the GaP nanowires. The crystal defects can be easily induced in the nanocables because of the presence of other elements during the growth. Therefore, the peak position of XRD and Raman spectrum shifts to the lower angle and the lower frequency region, respectively. In addition, the XPS, XRD, Raman spectrum, and PL spectrum consistently reveal that (1) the surface defects such as the doping and dangling bonds is significantly reduced by the outer layers, (2) the GaP/SiO_x

nanowires could be still doped with O atoms at the interface region, and (3) the GaP/SiO_x/C nanocables have more crystalline structure, probably due to the annealing effect at the C deposition temperature. The outer layer formation reduces the surface defects of GaP nanowires, so the fabrication of these nanocables would guarantee the reproducible electrical and optoelectrical properties of nanodevices.

The GaP nanowires sheathed with insulating SiO_x or metallic C outer layers would be useful for the interconnection in fabricating the nanoelectronic devices. The insulating effect of the SiO_x outer layers was confirmed by the conductivity measurement. The deposition of C outer layers greatly enhances the conductivity by reducing the contact resistance between the nanocables. Our result shows that the encapsulation with insulating and metallic outer layers can control the electrical properties of the nanostructures. Furthermore, the ends of individual GaP/SiO_x, GaP/C, and GaP/SiO_x/C nanocables are usually open, allowing one to make electrical contact by evaporation onto the wire end. The multishell coaxial nanocables have recently been a hot issue in nanoscience and nanotechnology. The Lieber group developed the nanosized coaxial transistor using the *p*-Si/*i*-Ge/SiO_x/*p*-Ge nanocables.[16] The synthesis of SiC/SiO_2/C or BN, Si/SiO_2/C or BN coaxial nanocables structure has been previously reported by several groups.[15,17a,18a,b] The present GaP/SiO_x/C nanocables would be an innovative material for nanoelectronic devices, because the insulating SiO_x layer isolates the semiconductor core from the metallic outer layers.

5. Conclusions

Three types of core−shell nanocables, GaP/SiO_x, GaP/C, and GaP/SiO_x/C, were fabricated successfully by controlling the condition of CVD. The keys of the synthesis methods are summarized as follows. (1) The coaxial GaP/SiO_x nanocables were produced directly on the Au nanoparticle-deposited Si substrates by CVD of ball-milled GaP powders and Si wafers as the Si source. (2) The amorphous C outer layers uniformly deposit on the GaP nanowires via the CVD of CH_4, following the sublimation of ball-milled GaP powders. (3) The graphitic outer layers uniformly form on the pregrown GaP/SiO_x nanocables via the CVD of C_2H_2.

The length of the nanocables is up to 500 μm. The GaP nanowire core consists of the zinc-blende structured crystals grown in the [111] direction. The thickness of the C outer layers is controlled by the C deposition time. The degree of crystalline perfection of the C outer layers increases with the deposition temperature. The effect of the outer layers on the structural properties of GaP nanowires was examined thoroughly using XPS, XRD, Raman spectroscopy, and PL. Although crystal defects are frequently produced during the growth process, the outer layers significantly reduce the surface defects of GaP nanowires by reducing the dangling bonds. We explained the growth process using the VLS mechanism. The conductivity measurement shows the effect of the insulating SiO_x and metallic C outer layers on the nanocables. These noble fabrications of the GaP core−shell nanocables with single or double shells in a controlled manner probably facilitate the building of a variety of nanodevices.

Supporting Information Available: Figure S1 shows the EDX data for GaP/SiO_x, GaP/C, and GaP/SiO_x/C nanocables. This material is available free of charge via the Internet at http://pubs.acs.org.

Acknowledgment. The KOSEF (project nos. R14-2003-033-0100-0, R02-2004-000-10025−0) and KRF (project no. 2003-015-C00265) supported the present work. SEM and X-ray diffraction analysis were performed at the Korea Basic Research Institute in Seoul. Experiments at PLS were supported in part by MOST and POSTECH.

References and Notes

(1) Duan, X.; Huang, Y.; Cui, Y.; Wang, J.; Lieber, C. M. *Nature (London)* **2001**, *409*, 66. (b) Gudiksen, M. S.; Duan, X.; Cui, Y.; Lieber, C. M. *Science* **2001**, *293*, 1455. (c) Huang, Y.; Duan, X.; Cui, Y.; Lauhon, L. J.; Kim, K.-H.; Lieber, C. M. *Science* **2001**, *294*, 1313. (d) Duan, X.; Huang, Y.; Agarwal, R.; Lieber, C. M. *Nature (London)* **2003**, *421*, 241.

(2) Tseng, G. Y.; Ellenbogen, J. C. *Science* **2001**, *294*, 1293.

(3) Melosh, N. A.; Boukai, A.; Diana, F.; Gerardot, B.; Badolato, A.; Petroff, P. M.; Heath, J. R. *Science* **2003**, *300*, 112.

(4) Xia, Y.; Yang, P.; Sun, Y.; Wu, Y.; Mayers, B.; Gates, B.; Yin, Y.; Kim, F.; Yan, H. *Adv. Mater.* **2003**, *15*, 353.

(5) Rao, C. N. R.; Deepak, F. L.; Gundiah, G.; Govindaraj, A. *Prog. Solid State Chem.* **2003**, *31*, 5.

(6) Hu, J.; Ouyang, M.; Yang, P.; Lieber, C. M. *Nature (London)* **1999**, *399*, 48.

(7) Zhang, Y.; Ichihashi, T.; Landree, E.; Nihey, F.; Iijima, S. *Science* **1999**, *285*, 1719.

(8) Park, W. I.; Yi, G. C.; Kim, M. Y.; Pennycook, S. J. *Adv. Mater.* **2003**, *15*, 526. (b) Jung, S. W.; Park, W. I.; Yi, G. C.; Kim, M. Y. *Adv. Mater.* **2003**, *15*, 1358.

(9) Luo, J.; Zhang, L.; Zhu, J. *Adv. Mater.* **2003**, *15*, 579.

(10) Nicewarner-Pena, S. R.; Freeman, R. G.; Reiss, B. D.; He, L.; Pena, D. J.; Walton, I. D.; Cromer, R.; Keating, C. D.; Natan, M. J. *Science* **2001**, *294*, 137.

(11) Gudiksen, M. S.; Lauhon, L. J.; Wang, J.; Smith, D. C.; Lieber, C. M. *Nature (London)* **2002**, *415*, 617. (b) Yu, Y.; Xiang, J.; Yang, C.; Lu, W.; Lieber, C. M. *Nature (London)* **2004**, *450*, 61.

(12) Wu, Y.; Fan, R.; Yang, P. *Nano Lett.* **2002**, *2*, 83.

(13) He, R.; Law, M.; Fan, R.; Kim, F.; Yang, P. *Nano Lett.* **2002**, *2*, 1109.

(14) Hu, J.; Bando, Y.; Liu, Z.; Sekiguchi, T.; Golberg, D.; Zhan, J. *J. Am. Chem. Soc.* **2003**, *125*, 11306.

(15) Zhang, Y.; Suenaga, K.; Colliex, C.; Iijima, S. *Science* **1998**, *281*, 973.

(16) Lauhon, L. J.; Gudiksen, M. S.; Wang, D.; Lieber, C. M. *Nature (London)* **2002**, *420*, 57.

(17) Shi, W.-S.; Peng, H.-Y.; Xu, L.; Wang, N.; Tang, Y.-H.; Lee, S.-T. *Adv. Mater*. **2000**, *12*, 1927. (b) Sun, X.-H.; Li, C.-P.; Wong, W.-K.; Wong, N.-B.; Lee, C.-S.; Lee, S.-T.; Teo, B.-K. *J. Am. Chem. Soc.* **2002**, *124*, 14464. (c) Hu, J.-Q.; Meng, X.-M.; Jiang, Y.; Lee, C.-S.; Lee, S.-T. *Adv. Mater*. **2003,** *15*, 70. (d) Meng, X.-M.; Hu, J.-Q.; Jiang, Y.; Lee, C.-S.; Lee, S.-T. *Appl. Phys. Lett.* **2003**, *83*, 2241. (e) Teo, B. K.; Li, C. P.; Sun, X. H.; Wong, N. B.; Lee, S. T. *Inorg. Chem.* **2003**, *42*, 6723.

(18) Zhu, Y.-C.; Bando, Y.; Xue, D.-F.; Xu, F.-F.; Golberg, D. *J. Am. Chem. Soc.* **2003**, *125*, 14226. (b) Li, Y.; Bando, Y.; Golberg, D. *Adv. Mater*. **2004**, *16*, 93. (c) Tang, C. C.; Bando, Y.; Sato, T.; Kurashima, K. *Adv. Mater.* **2002**, *14*, 1046. (d) Gao, Y.; Bando, Y.; Golberg, D. *Appl. Phys. Lett.* **2002**, *81*, 4133. (e) Hu, J.; Bando, Y.; Liu, Z. *Adv. Mater*. **2003**, *15*, 1000. (f) Tang, C.; Bando, Y.; Golberg, D.; Ding, X.; Qi, S. *J. Phys. Chem. B* **2003**, *107*, 6539. (g) Li, Y. B.; Bando, Y.; Golberg, D.; Liu, Z. W. *Appl. Phys. Lett*. **2003**, *83*, 999. (h) Golberg, D.; Bando, Y.; Fushimi, K.; Mitome, M.; Bourgeois, L.; Tang, C. C. *J. Phys. Chem. B* **2003**, *107*, 8726. (i) Zhu, Y. C.; Bando, Y.; Ma, R.-Z. *Adv. Mater*. **2003**, *15*, 1377. (j) Gao, Y.; Bando, Y.; Liu, Z.; Golberg, D.; Nakanishi, H. *Appl. Phys. Lett.* **2003**, *83*, 2913. (k) Li, Y. B.; Bando, Y.; Golberg, D.; Uemura, Y. *Appl. Phys. Lett*. **2003**, *83*, 3999. (l) Yin, L. W.; Bando, Y.; Zhu, Y. C.; Li, M. S. *Appl. Phys. Lett.* **2004**, *84*, 5314.

(19) Wang, X.; Gao, P.; Li, J.; Summers, C. J.; Wang, Z. L. *Adv. Mater*. **2002**, *14*, 1732. (b) Ding, Y.; Kong, X. Y.; Wang, Z. L. *J. Appl. Phys.* **2004**, *95*, 306. (c) Kong, X. Y.; Ding, Y.; Wang, Z. L. *J. Phys. Chem. B* **2004**, *108*, 570.

(20) Han, W.; Zettl, A. *Adv. Mater*. **2002**, *14*, 1560. (b) Han, W.; Zettl, A. *Appl. Phys. Lett.* **2002**, *81*, 5051.

(21) Wu, Y.; Yang, P. *Appl. Phys. Lett.* **2000**, *77*, 43. (b) Wu, Y.; Yang, P. *Adv. Mater.* **2001**, *13*, 520. (c) Choi, H.-J.; Johnson, J. C.; He, R.; Lee, S.-K.; Kim, F.; Pauzauskie, P.; Goldberger, J.; Saykally, R. J.; Yang, P. *J. Phys. Chem. B* **2003**, *107*, 8721.

(22) Yin, Y.; Lu, Y.; Sun, Y.; Xia, Y. *Nano Lett*. **2002**, *2*, 427. (b) Jiang, X.; Mayers, B.; Herricks, T.; Xia, Y. *Adv. Mater.* **2003**, *15*, 1740.

(23) Wu, J.-J.; Liu, S.-C.; Wu, C.-T.; Chen, K.-H.; Chen, L.-C. *Appl. Phys. Lett.* **2002**, *81*, 1312. (b) Wu, J.-J.; Wong, T.-C.; Yu, C.-C. *Adv. Mater.* **2002**, *14*, 1643.

(24) Seo, H. W.; Bae, S. Y.; Park, J.; Yang, H.; Kim, B. *J. Phys. Chem. B* **2003**, *107*, 6739. (b) Kim, H. Y.; Bae, S. Y.; Kim, N. S.; Park, J. *Chem. Commum.* **2003**, *20*, 2634.

(25) Obare, S. O.; Jana, N. R.; Murphy, C. J. *Nano Lett.* **2001**, *1*, 601.

(26) Manna, L.; Scher, E. C.; Li, L.-S.; Alivisatos, A. P. *J. Am. Chem. Soc.* **2002**, *124*, 7136.
(27) Zhang, Y.; Wang, N.; Gao, S.; He, R.; Miao, S.; Liu, J.; Zhu, J.; Zhang, X. *Chem. Mater.* **2002**, *14*, 3564.
(28) Hofmann, S.; Ducati, C.; Robertson, J. *Adv. Mater.* **2002**, *14*, 1821.
(29) Zhu, Y. Q.; Hsu, W. K.; Kroto, H. W.; Walton, D. R. M. *J. Phys. Chem. B* **2002**, *106*, 7623.
(30) Lin, H.-M.; Chen, Y.-L.; Yang, J.; Liu, Y.-C.; Yin, K.-M.; Kai, J.-J.; Chen, F.-R.; Chen, L.-C.; Chen, Y.-F.; Chen, C.-C. *Nano Lett.* **2003**, *3*, 537.
(31) Guo, Y.-G.; Wan, L.-J.; Bai, C.-L. *J. Phys. Chem. B* **2003**, *107*, 5441.
(32) Kolmakov, A.; Zhang, Y.; Moskovits, M. *Nano Lett.* **2003**, *3*, 1125.
(33) Kovtyukhova, N. I.; Mallouk, T. E.; Mayer, T. S. *Adv. Mater.* **2003**, *15*, 780.
(34) Li, Q.; Wang, C. *J. Am. Chem. Soc.* **2003**, *125*, 9892.
(35) Hsia, C.-H.; Yen, M.-Y.; Lin, C.-C.; Chiu, H.-T.; Lee, C.-Y. *J. Am. Chem. Soc.* **2003**, *125*, 9940.
(36) Jiang, Z.-Y.; Xie, Z.-X.; Zhang, X.-H.; Huang, R.-B.; Zheng, L.-S. *Chem. Phys. Lett.* **2003**, *378*, 313.
(37) Mokari, T.; Banin, U. *Chem. Mater.* **2003**, *15*, 3955.
(38) Cao, J.; Sun, J.-Z.; Hong, J.; Li, H.-Y.; Chen, H.-Z.; Wang, M. *Adv. Mater.* **2004**, *16*, 84.
(39) Geng, B.; Meng, G.; Zhang, L.; Wang, G.; Peng, X. *Chem. Commun.* **2003**, *20*, 2572.
(40) Liang, C.; Shimizu, Y.; Sasaki, T.; Umehara, H.; Koshizaki, N. *J. Mater. Chem.* **2004**, *14*, 248.
(41) Han, S.; Li, C.; Liu, Z.; Lei, B.; Zhang, D.; Jin, W.; Liu, X.; Tang, T.; Zhou, C. *Nano Lett.* **2004**, *4*, 1241.
(42) Liang, X.; Tan, S.; Tang, Z.; Kotov, N. A. *Langmuir* **2004**, *20*, 1016.
(43) Hwang, J.; Min, B.; Lee, J. S.; Keem, K.; Cho, K.; Sung, M.-Y.; Lee, M. S.; Kim, S. *Adv. Mater.* **2004**, *16*, 422.
(44) Dai, L.; Chen, X. L.; Zhang, X.; Zhou, T.; Hu, B. *Appl. Phys. A* **2004**, *78*, 557.
(45) Duan, X.; Lieber, C. M. *Adv. Mater.* **2000**, *12*, 298.
(46) Shi, W. S.; Zheng, Y. F.; Wang, N.; Lee, C. S.; Lee, S. T. *J. Vac. Sci. Technol., B* **2001**, *19*, 1115.
(47) Tang, C.; Fan, S.; Lamy de la Chapelle, M.; Dang, H.; Li, P. *Adv. Mater.* **2000**, *12*, 1346.
(48) Kim, Y.-H.; Jun, Y.-W.; Jun, B.-H.; Lee, S.-M.; Cheon, J. *J. Am. Chem. Soc.* **2002**, *124*, 13656.
(49) Lyu, S. C.; Zhang, Y.; Ruh, H.; Lee, H. J.; Lee, C. J. *Chem. Phys. Lett.* **2003**, *367*, 717.
(50) Seo, H. W.; Bae, S. Y.; Park, J.; Yang, H. Kim, S. *Chem. Commun.* **2002**, 2564.
(51) Seo, H. W.; Bae, S. Y.; Park, J.; Yang, H.; Kang, M.; Kim, S. *Appl. Phys. Lett.* **2003**, *82*, 3752.
(52) Seo, H. W.; Bae, S. Y.; Park, J.; Kang, M.; Kim, S. *Chem. Phys. Lett.* **2003**, *378*, 420.
(53) Moulder, J. F.; Stickle, W. F.; Sobol, P. E.; Bomben, K. D. *Handbook of X-ray Photoelectron Spectroscopy*; Chastain, J., King, R. C., Jr., Eds.; Physical Electronics, Inc.: Eden Prairie, MN, 1992.
(54) Nasibov, A. S.; Mel'nik, N. N.; Ponomarev, I. V.; Romanko, S. V.; Topchii, S. B.; Obraztsov, A. N.; Yu Bashtanov, M.; Krasnovskii, A. A. *Quantum Electron.* **1998**, *28*, 40.
(55) Gupta. R.; Xiong, Q.; Mahan, G. D.; Eklund, P. C. *Nano Lett.* **2003**, *3*, 1745.
(56) Mahan, G. D.; Gupta, R.; Xiong, Q.; Adu, C. K.; Eklund, P. C. *Phys. Rev. B* **2003**, *68*, 073402.
(57) Tuinstra, F.; Koenig, J. L. *J. Chem. Phys.* **1970**, *53*, 1126.
(58) Massalski, T. B.; Okamoto, H.; Subramanian, P. R.; Kacprozak, L. *Binary Alloy Phase Diagrams*, 2nd ed.; American Society for Metals: Metals Park, OH, 1992.
(59) Pan, Z. W.; Dai, Z. R.; Ma, C.; Wang, Z. L. *J. Am. Chem. Soc.* **2002**, *124*, 1817.
(60) Zheng, B.; Wu, Y.; Yang, P.; Liu, J. *Adv. Mater.* **2002**, *14*, 122.
(61) Kim, H. Y.; Park, J.; Yang, H. *Chem. Commun.* **2002**, *2*, 256.